LA-UR- 09-04965

*Approved for public release;*
*distribution is unlimited.*

| | |
|---|---|
| *Title:* | Current Pulse Effects on Cylindrical Damage Experiments |
| *Author(s):* | Ann Kaul, X-1-SMMP<br>Christopher Rousculp, X-1-PTA |
| *Intended for:* | Proceedings of IEEE Pulsed Power Conference 2009<br>Washington, D.C.<br>June 28 - July 2, 2009 |

Los Alamos
NATIONAL LABORATORY
EST. 1943



Form 836 (7/06)

# CURRENT PULSE EFFECTS ON CYLINDRICAL DAMAGE EXPERIMENTS

**A. M. Kaul, C. L. Rousculp**
Los Alamos National Laboratory, P.O. Box 1663, MS-F699
Los Alamos, NM, USA

*Abstract*

A series of joint experiments between LANL and VNIIEF use a VNIIEF-designed helical generator to provide currents for driving a LANL-designed cylindrical spallation experimental load. Under proper driving conditions, a cylindrical configuration allows for a natural recollection of the damaged material. In addition, the damaged material is able to come to a complete stop due to its strength, avoiding application of further forces. Thus far, experiments have provided data about failure initiation of a well-characterized material (aluminum) in a cylindrical geometry, behavior of material recollected after damage from pressures in the damage initiation regime, and behavior of material recollected after complete failure. In addition to post-shot collection of the damaged target material for subsequent metallographic analysis, dynamic in-situ experimental diagnostics include velocimetry and transverse radial radiography. This paper will focus on the effects of tailoring the driving current pulse to obtain the desired data.

## I. INTRODUCTION

A series of ten spallation damage experiments, designated R-Damage, are being executed jointly by Los Alamos National Laboratory (LANL) and the All Russian Scientific Institute of Experimental Physics (VNIIEF). The experiments use VNIIEF's explosively-driven electro-magnetic generators to drive LANL-designed experimental loads. Eight of these experiments have been completed. These experiments addressed the difference in damage initiation between planar and cylindrical geometry and studied the behavior of material recollected after damage produced with pressures in this damage initiation range. The objectives of the experiments have been met with varying degrees of success. This paper will show how the accuracy of prediction of the driving current pulse becomes more important as the physics of the experiment becomes more complicated.

## II. EXPERIMENTAL DESIGN

The R-Damage experiments study damage in an inner cylindrical shell (target) impacted by an outer cylindrical shell (liner) launched by the magnetic pressure force ($j \times B$) generated when an axial current is sent along the outer liner wall. Liner impact with the target launches a pressure wave through the target. The amount of damage produced in the target depends on liner impact velocity and thickness of the target. The driving current and location of the target control liner impact velocity.

Liner and target material for these experiments was a high-purity extruded aluminum. Each load contained two targets. Targets varied in the radial direction to produce varying peak free surface velocities and damage conditions from the same drive conditions.

Electro-magnetic drivers provide a unique opportunity to study controlled compression in a convergent geometry. One major advantage of a magnetically-driven system, crucial to spallation damage experiments, is the ability to recover the load for post-experiment metallurgical analysis. Recovered samples provide grain-scale data such as void and void cluster sizes, final sample porosity profile and final sample volume void number density profile for use in model development.

The VNIIEF assembly had a shield between the explosive generator and the load region, allowing recovery of targets for metallurgical examination and damage quantification. Photon doppler velocimetry (PDV) recorded the inner free surface velocity of the targets and of the moving liner, using two probes at each recording position. The liner velocity can be used to infer impact conditions, while the target velocities can be used to infer the pressure wave profile after transit of the entire target thickness. Faraday inductive loops and B-dot probes were used to measure driving currents in the load, the generator and the transmission lines.

## II. CASE I

The first case involves the experiments designated R-Damage-0, -1 and -2. These experiments were designed to obtain incipient spall, i.e. void formation and growth but no complete failure, in a cylindrical geometry. The range of pressures which produce such behavior is quite small. The corresponding impact velocity range is also quite small, with a difference of 12 m/s between no voids and complete failure in the planar case. Thus, for these experiments, control of the impact velocity was critical.

**Table 1.** Expected impact velocity and time and peak free surface velocity and time for RD-0 and –1 targets.

| Max Current (MA) | Impact Velocity (m/s) and Time (μs) @ r=45 mm | | FS Velocity (m/s) and Time (μs) @ r=25 mm | | Impact Velocity (m/s) and Time (μs) @ r=44 mm | | FS Velocity (m/s) and Time (μs) @ r=24 mm | | Impact Velocity (m/s) and Time (μs) @ r=43 mm | | FS Velocity (m/s) and Time (μs) @ r=23 mm | |
|---|---|---|---|---|---|---|---|---|---|---|---|---|
| 4.754 | 192.8 | 20.52 | 202.8 | 24.58 | 187.7 | 25.78 | 200.1 | 29.84 | 181.9 | 31.18 | 196.4 | 35.24 |
| 4.802 | 197.4 | 20.18 | 208.9 | 24.24 | 192.5 | 25.32 | 206.4 | 29.38 | 186.8 | 30.58 | 203.0 | 34.64 |
| 4.851 | 202.1 | 19.86 | 214.9 | 23.92 | 197.2 | 24.88 | 212.7 | 28.92 | 191.8 | 30.00 | 209.6 | 34.06 |
| 4.900 | 206.8 | 19.56 | 221.0 | 23.60 | 202.2 | 24.44 | 219.0 | 28.50 | 196.8 | 29.46 | 216.1 | 33.50 |
| 4.948 | 211.5 | 19.26 | 227.1 | 23.28 | 206.9 | 24.04 | 225.3 | 28.06 | 201.8 | 28.92 | 222.7 | 32.96 |
| 4.997 | 216.3 | 18.96 | 233.3 | 23.00 | 211.8 | 23.64 | 231.7 | 27.66 | 206.8 | 28.40 | 229.4 | 32.44 |
| 5.045 | 221.1 | 18.68 | 239.5 | 22.70 | 216.7 | 23.26 | 238.1 | 27.28 | 211.8 | 27.92 | 236.0 | 31.94 |

### *A. Design Process*

Due to time constraints, the generator and the load were designed in a parallel process. Thus, an "ideal" current was chosen as a target. This current is shown in Fig. 1. It consists of a 2 μs rise time to the peak current, a flat current for 6 μs and a 2 μs fall back to zero current. The relatively sharp rise and fall of the current were accomplished using switches to control the current in the load region. This short pulse needed to accelerate the liner to an appropriate velocity, at which point the current would be removed and the liner allowed to continue in free flight. This design mimicked a planar gas gun-driven flyer plate impact.

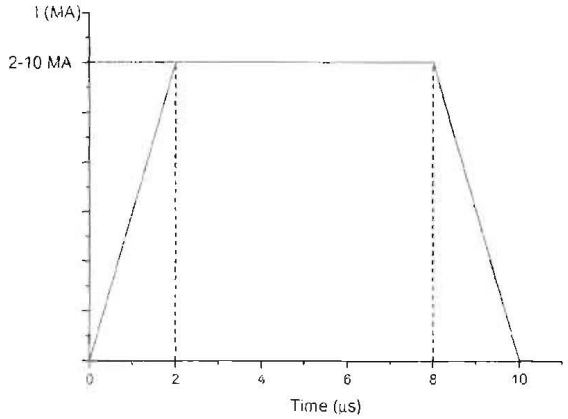


**Figure 1.** RD-0, -1, -2 "ideal" current.

With this configuration, the peak current is the sole input parameter of the generator. A liner thickness and radius were chosen to match previous experiments. Calculations of the liner velocity over a range of peak currents were completed, with the results for peak currents of 4.8, 5.0, 5.2 and 5.4 MA shown in Fig. 2 and Fig. 3. Velocity is plotted as a function of liner radius in Fig. 2 and as a function of time in Fig. 3. Velocity is negative since the liner is converging on center. In both plots, black horizontal lines indicate the range of incipient spall for the planar case and the desired liner velocity range. Note that the peak velocity corresponds to the end of the current pulse, after which the liner slows as strength resists convergence.

The calculations showed that too little current did not produce enough velocity, while too much current reduced to an appropriate velocity at a very small radius and very late time. It appeared that targets placed at a radius of 43 to 45 mm could be reached at a reasonable time of 15 to 30 μs using a 5.0 MA peak current. It also appeared that liner impact velocity and time were basically linear functions of the peak current. More refined calculations with peak currents between 4.75 and 5.05 MA were completed to determine impact time and velocity for targets placed at 43, 44 and 45 mm radii. The results are shown in Table 1, along with the expected target free surface shock breakout velocity. These numbers showed that, given a target location, it was relatively easy to produce a chosen impact or free surface breakout velocity by changing the peak current.

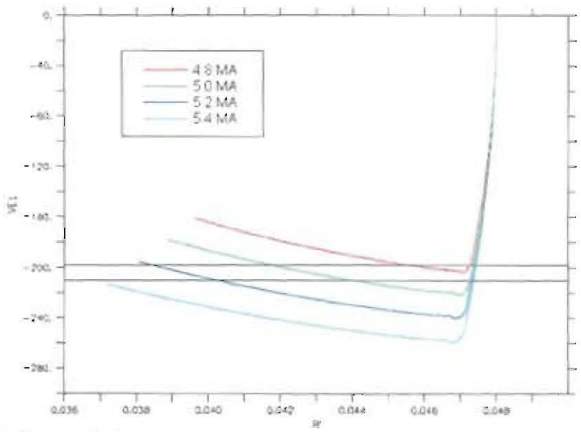


**Figure 2.** Velocity as a function of radius for 4.8, 5.0, 5.2 and 5.4 MA. Horizontal lines indicate targeted range.

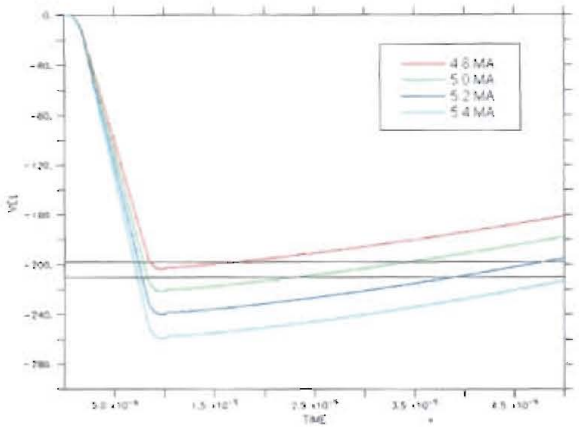


**Figure 3.** Velocity as a function of time for 4.8, 5.0, 5.2 and 5.4 MA. Horizontal lines indicate targeted range.

### *B. RD-0 Experiment*

The chosen outer target radius for the RD-0 experiment was 44 mm, with the inner radius at 24 mm. This is the middle case in Table 1. For the expected 5.0 MA peak current, the target's free surface peak velocity was expected to be 232 m/s. The measured current for the experiment is shown in Fig. 4. It can be seen that the current pulse was basically as expected. The measured target free surface velocity, shown in Fig. 5, had a peak free surface velocity of 252 m/s, higher than anticipated and causing formation of a complete damage surface, as shown in the metallographic result shown in Fig. 6. Clearly, the peak current needed to be reduced in the later experiments to obtain the desired damage state.

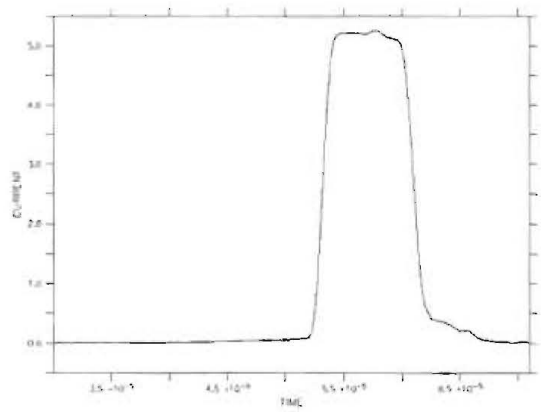

**Figure 4.** RD-0 measured current.

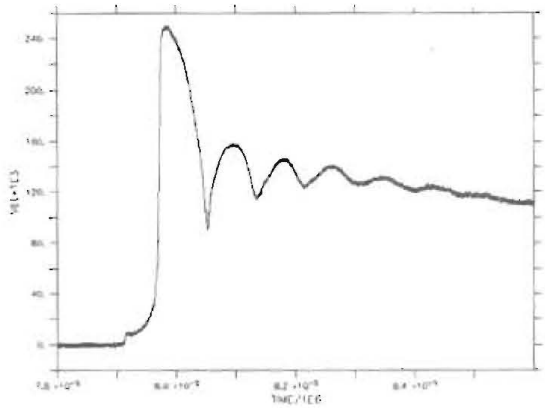

**Figure 5.** RD-0 measured target free surface velocity.

**Figure 6.** RD-0 target metallography of damage surface area.

It was estimated that the target free surface velocity should be reduced to 200 to 210 m/s to obtain only void formation. In addition, the outer radii of the targets in the second experiment were 43 and 45 mm, with inner radii of 23 and 25 mm. These are the first and third cases in Table 1. After adjusting for the differences in radii and desired velocity, the peak current was reduced by 10 percent to 4.5 MA for the second experiment.

### *C. RD-1 Experiment*

The measured current for the RD-1 experiment is shown in Fig. 7. While it has the same basic shape as the RD-1 current, the peak value has been reduced. The measured free surface velocity of the 45 mm radius target is shown in Fig. 8, with the corresponding metallographic result shown in Fig. 9. For the 43 mm radius target, the measured free surface velocity is shown in Fig. 10, with the metallographic result shown in Fig. 11. With the reduced peak free surface velocities, the damage state was reduced to the formation of voids and partial coalescence in Fig. 9 and the beginning of crack formation in Fig. 11. Thus, the desired outcome of the experiments was obtained. This case shows that when the experimental physics is simple enough, some difference from the expected driving current results can be successfully accommodated.

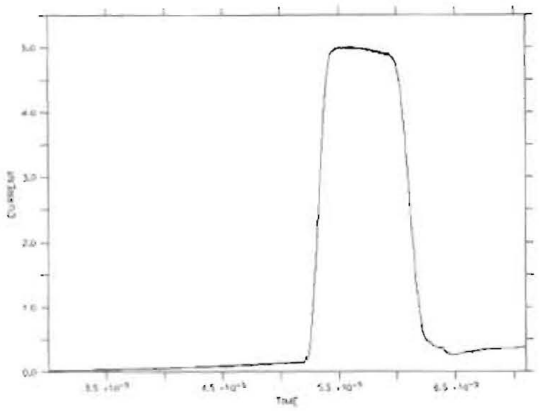

**Figure 7.** RD-1 measured current.

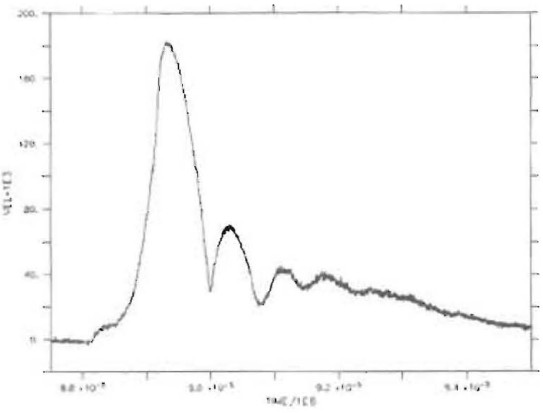

**Figure 8.** RD-1 45 mm target free surface velocity.

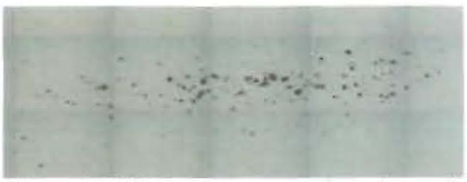

**Figure 9.** RD-1 45 mm target metallography.

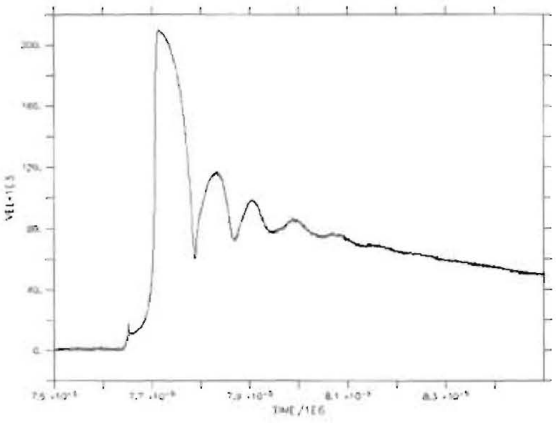

**Figure 10.** RD-1 43 mm target free surface velocity.

**Figure 11.** RD-1 43 mm target metallography.

## III. CASE II

The second case involves the RD-6 and -7 experiments. In these two experiments, the physics objective became much more complicated. The goal of these experiments was to have the liner impact the target hard enough to form a complete crack, then reaccelerate and recollect the spalled layer, then stop before collapsing to center. This required a continued drive on the liner after impact, with current removal at the appropriate time. A larger radius liner and target were needed to obtain the desired results, so a larger generator was also needed. The chosen "ideal" current is shown in Fig. 12. It consists of a 2 μs rise time to the peak current, a slightly dropping current for 40 μs and a 4 to 8 μs fall back to zero current.

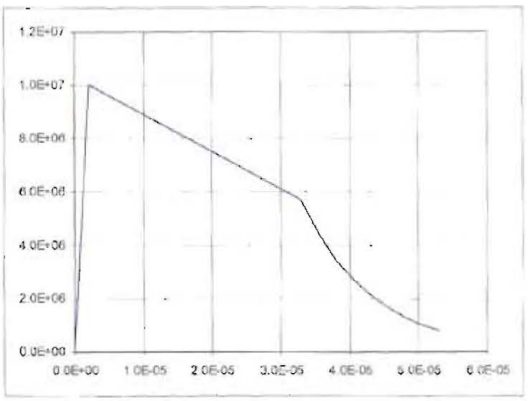


**Figure 12.** RD-6, -7 "ideal" current.

Any target peak free surface velocity of more than 200 m/s would result in formation of a complete fracture surface. Calculations using a peak current of 7, 8, 9 and 10 MA were completed, with the results shown in Table 2. As the numbers show, any of these currents should be able to produce the complete fracture condition. Then the question becomes whether the assembly will stop before it collapses to the center. Calculations with a 10 MA peak current showed complete spall, recollection and the assembly stopping at 12 mm for one target and 13 mm for the second target. It should be noted that these stopping distances are highly dependent on the chosen strength model. However, the 10 MA case is the worst case, so reducing the current was expected to improve the stopping radius.

**Table 2.** Target peak free surface velocity.

| Peak Current | 56 mm Peak FS Velocity | Time | 55.5 mm Peak FS Velocity | Time |
|---|---|---|---|---|
| 7 MA | 253.4 | 12.04 | 296.5 | 14.14 |
| 8 MA | 296.8 | 10.84 | 348.6 | 12.64 |
| 9MA | 341.3 | 9.94 | 401.0 | 11.5 |
| 10 MA | 385.6 | 9.22 | 452.8 | 10.62 |

### *A. Generator Test*

The generator was a new design, so a "static" load test was performed. The equivalent current for the dynamic load was then calculated, with the result shown in pink and the "ideal" current shown in navy in Fig. 13. The adjusted measured current was slightly higher than the ideal current at early times, which would push the liner faster than expected, resulting in a higher impact velocity for a given target radius. This could be countered by reducing the peak current slightly. The adjusted measured current, however, was lower at later times, providing less energy for reacceleration and recollection of the spall layer. Comparisons between codes did not agree on whether the assembly would be able to stop, so a second static test was performed using an 8.5 MA peak current. After adjusting for a dynamic load, calculations showed that both targets were expected to spall, one target was definitely expected to recollect, partial recollection was expected in the second target and both targets were expected to stop.

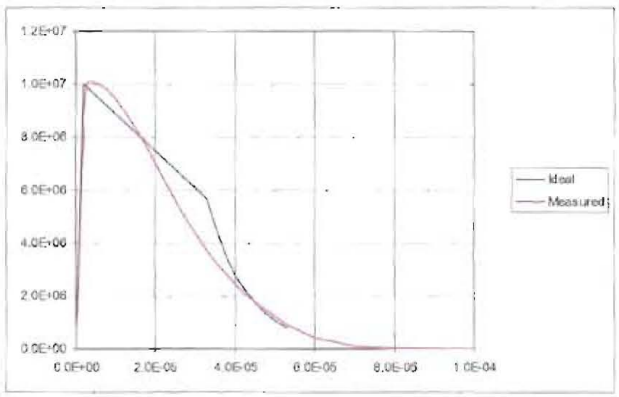


**Figure 13.** Adjusted measured current in pink, "ideal" current in navy.

### *B. RD-7 Experiment*

The RD-7 experiment was conducted with an expected peak current of 8.2 MA. The measured current is shown in Fig. 14. While the peak current was reasonably accurate, it can be seen that the current does not reduce to zero at late time. The measured free surface velocities of the two targets are shown in Fig. 15 and Fig. 16. Both traces show a shock wave arriving at the free surface followed by a typical spallation signal and ringing of the spalled layer. This is followed by a reacceleration caused by the recollecting liner, after which is seen more ringing and acceleration of the assembly towards the center. Thus, while the goal of complete spall and recollection was obtained, the unexpectedly long tail on the current caused the assembly to collapse to the center. This case shows that as the experimental physics becomes more complex and integrated, accommodation of differences in the expected and obtained current becomes more difficult, sometimes impossible.

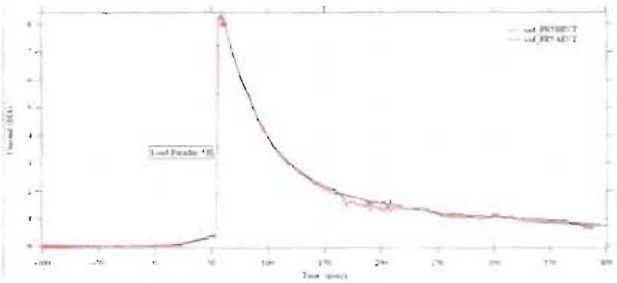

**Figure 14.** RD-7 measured current.

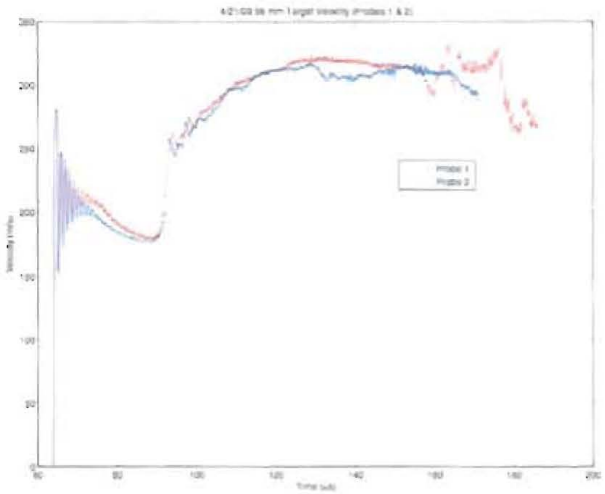

**Figure 15.** RD-7 56 mm target free surface velocity.

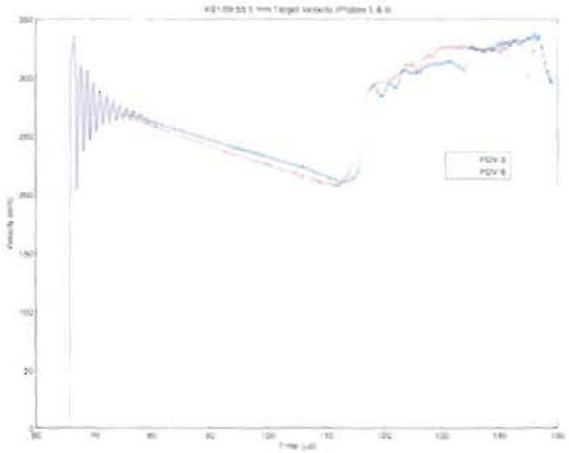

**Figure 16.** RD-7 55.5 mm target free surface velocity.

## IV. CONCLUSIONS

For the designer of experiments, an adequate description of the driving conditions produced by a experimental device is crucial prior to designing the experiment. Typically, some part of the experimental assembly is designed from the expected drive conditions. For the R-Damage experiments, the expected shape of the current pulse decided the locations of the targets. Once the experimental assembly is completed, the only changeable piece available in the experiment is the drive condition. If the experimental physics is simple enough, some difference from the expected driving condition can be successfully accommodated, as evidenced by the R-Damage-0, -1 & -2 series. As the experimental physics becomes more complex and integrated, accommodation becomes more difficult. Sometimes the difference is such that it becomes impossible to achieve all of the experimental goals with any given available drive, as in the R-Damage-6 & -7 series.

## V. Acknowledgements

The authors thank all members of the LANL and VNIIEF experimental teams whose capable work make these experiments possible.